CHALMERS
UNIVERSITY OF TECHNOLOGY

25-GBd 850-nm VCSEL for an Extended Temperature Range

Citation for the original published paper (version of record):
Kaimre, H., Grabowski, A., Gustavsson, J. et al (2025). 25-GBd 850-nm VCSEL for an Extended Temperature Range. IEEE Photonics Technology Letters, 37(6): 369-372.
http://dx.doi.org/10.1109/LPT.2025.3547156

(article starts on next page)

This article has been accepted for publication in IEEE Photonics Technology Letters. This is the author's version which has not been fully edited and content may change prior to final publication. Citation information: DOI 10.1109/LPT.2025.3547156.

25 Gbaud 850 nm VCSEL for an Extended Temperature Range

Hans Daniel Kaimre, Alexander Grabowski, Johan Gustavsson, and Anders Larsson

***Abstract*—We investigate the performance of a 25 Gbaud 850 nm vertical-cavity surface-emitting laser (VCSEL) with reduced temperature dependence from −40 to 125 °C. The VCSEL design implements chirped quantum wells (QWs) with different compositions to broaden the gain spectrum and achieve sufficient performance over the entire temperature range at constant bias current and modulation voltage. A 6 µm oxide aperture diameter VCSEL supports data transmission at 25 Gb/s NRZ from −40 to 125 °C with 8 mA bias current and 640 mV modulation voltage. The temperature dependencies of basic performance parameters are also compared to those of a conventional VCSEL with identical QWs.**

***Index Terms*—Vertical-cavity surface-emitting laser, dynamics, temperature dependence.**

I. Introduction

THE vertical-cavity surface-emitting laser (VCSEL) is the preferred light source for high-speed and power-efficient short-reach optical interconnects (OIs) in high-performance computing systems, datacenters, and other short-range optical networks [1]. Such OIs typically operate over a temperature range of 0 to 70 °C. However, some emerging applications of VCSEL-based OIs, such as in automotive optical networking [2] and optical networks in some military systems, require operation over a much wider temperature range, e.g. from −40 to 125 °C. With the VCSEL being the most temperature sensitive component of the OI, and uncooled/unheated operation required for cost and power efficiency, there is a demand for VCSELs with reduced temperature dependence, operating over a wider temperature range. Reduced temperature dependence and improved VCSEL performance at high temperatures would also benefit co-packaging of VCSEL-based optical transceivers in high-performance computing systems [3].

Manuscript received November 7, 2024; revised December 11, 2024; accepted 22 February 2025. Date of publication 27 February 2025; date of current version 27 February 2025. It was supported by the Swedish Foundation for Strategic Research under project HOT-OPTICS, CHI19-0004. *(Corresponding author: H. D. Kaimre.)*

H. D. Kaimre is with the Photonics Laboratory, Department of Microtechnology and Nanoscience, Chalmers University of Technology, SE-412 96 Gothenburg, Sweden (e-mail: kaimre@chalmers.se).

A. Grabowski was with the Photonics Laboratory, Department of Microtechnology and Nanoscience, Chalmers University of Technology, SE-412 96 Gothenburg, Sweden. He is now with Iloomina AB, SE-433 34 Partille, Sweden (e-mail: agrabowski@iloomina.com).

J. Gustavsson and A. Larsson were with the Photonics Laboratory, Department of Microtechnology and Nanoscience, Chalmers University of Technology, SE-412 96 Gothenburg, Sweden. They are now with NVIDIA, SE-417 55 Gothenburg, Sweden (e-mail: jgustavsson@nvidia.com; alarsson@nvidia.com).

Color versions of one or more figures in this letter are available at https://doi.org/10.1109/LPT.2025.3547156.

Digital Object Identifier 10.1109/LPT.2025.3547156

Variations of VCSEL performance over temperature is to a large extent caused by variations of optical gain and differential gain in the active region through temperature dependent Fermi occupation probabilities. The temperature dependence is further accelerated by the different rates at which the gain spectrum and resonance (lasing) wavelengths red-shift with increasing temperature. Therefore, previous attempts to reduce temperature dependence have used techniques to spectrally broaden the optical gain, e.g. different thickness quantum wells (QWs) [4]–[6] or quantum dots (QDs) with a size distribution [7] in the active region, where different size QWs and QDs produce optical gain at different wavelengths, thus broadening the overall gain.

In this Letter, we report on the design and performance of a 25 Gbaud class 850 nm VCSEL with reduced temperature dependence through the use of chirped QWs. In contrast to previous work, the QWs are chirped by varying the composition rather than the thickness. We demonstrate low temperature dependence of threshold current, modulation bandwidth, and damping of the modulation response from −40 to 125 °C. Eye diagrams recorded under 25 Gb/s NRZ large-signal modulation over temperature are also presented. In addition, basic performance characteristics are compared to those of a reference VCSEL with equal composition QWs, but otherwise identical. This work, to our knowledge, is the first to report such data rates for an 850 nm datacom VCSEL with chirped QWs in the active region over an extended temperature range from −40 to 125 °C.

II. VCSEL Design and Fabrication

The 850 nm VCSEL design is a modified version of the high-speed VCSEL design presented in [8] with 2 + 4 oxide layers for reduced capacitance. The smaller aperture in the two oxide layers closest to the active region provides transverse current and optical confinement. The active region consists of five 4 nm thick strained $In_xGa_{1-x}As/Al_{0.37}Ga_{0.63}As$ QWs for high differential gain. To avoid interband absorption in the low-index AlGaAs layers in the distributed Bragg reflectors (DBRs) at the highest temperatures, the Al-content was increased from 12 to 14 %.

For an 850 nm VCSEL, the gain spectrum red-shifts at a rate of approximately 0.33 nm/°C with increasing temperature because of a reduction of the band gap. The resonance wavelength, however, red-shifts at a rate of only about 0.07 nm/°C, mainly set by the temperature dependence of the refractive indices of the layers in the VCSEL cavity. This mismatch has to be accounted for when designing the VCSEL for required performance over a certain temperature range.

This article has been accepted for publication in IEEE Photonics Technology Letters. This is the author's version which has not been fully edited and content may change prior to final publication. Citation information: DOI 10.1109/LPT.2025.3547156.

Most VCSEL performance parameters at a given bias current degrade with increasing threshold current and the temperature dependencies of these parameters are strongly correlated with the temperature dependence of the threshold current [9]. Variations of threshold current with temperature should thus be kept at a minimum and excessive threshold current at the temperature endpoints should be avoided. Our VCSEL design, with different composition QWs, therefore aims at minimizing threshold current variations over the temperature range −40 to 125 °C. The design process is explained in the following text.

First, the quasi-Fermi level separation (QFLS) and the gain spectrum were calculated for different composition 4 nm thick $In_xGa_{1-x}As/Al_{0.37}Ga_{0.63}As$ QWs at different carrier densities and temperatures using SimuLase [10]. Then, 1D transfer matrix method (TMM) resonator simulations were used to calculate the resonance wavelength, the optical confinement factor for each of the QWs, and the modal gain at threshold at the different temperatures. Temperature dependent optical loss, caused by temperature dependent free carrier absorption in the DBRs, was accounted for. Next, for a set of QWs with given compositions, and under the assumption of mutual thermal equilibrium (i.e. a single set of quasi-Fermi levels to represent the population of states in all QWs), the QFLS was increased until the modal gain reached threshold. This was done over temperature and at each temperature the carrier density in the QWs at threshold was monitored.

At threshold, carrier injection balances spontaneous carrier recombination in the QWs. Under the assumption that carrier recombination is dominated by spontaneous emission, threshold current becomes proportional to threshold carrier density squared. Therefore, we use the sum of threshold carrier densities squared in the QWs as a measure of threshold current. An algorithm was developed to systematically search for the combination of QW compositions that minimized the variation of this quantity from −40 to 125 °C. Over 100 000 different combinations were examined. The final design, with a resonance wavelength of 847.5 nm at room temperature (RT, 20 °C) had QWs with calculated RT photoluminescence (PL) peak wavelengths at 822.2, 830.9, 846.0, 826.0, and 817.4 nm. At −40 °C, the longest wavelength (highest In-content) QW provides most of the optical gain. With increasing temperature, the other QWs contribute sequentially, while at 125 °C the shortest wavelength (lowest In-content) QWs provide most of the gain.

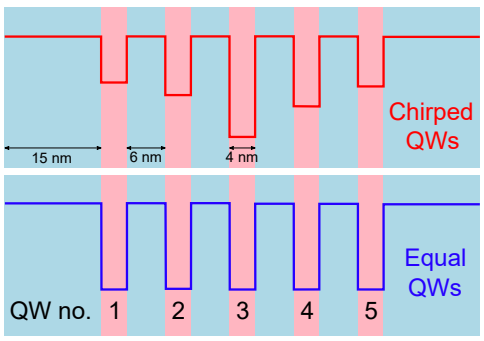

Fig. 1. Active region QW design for the VCSEL with chirped QWs (top) and the reference VCSEL with equal QWs (bottom). Energy levels not to scale.

In addition to the design with chirped QWs, a design with equal QWs was developed for comparison. These QWs had an RT PL wavelength of 834 nm, and therefore a detuning of 13.5 nm which should result in minimum threshold current at approximately 40 °C. The two active region designs are illustrated in Fig. 1.

The epitaxial VCSEL wafers were produced by metal-organic chemical vapor deposition at JENOPTIK Optical Systems GmbH. Active region calibrations were used to tune the different In-contents in the QWs. A RT active region PL spectrum for the VCSEL with chirped QWs is shown in Fig. 2. Also shown are the simulated PL spectra for the different QWs using SimuLase, as well as the sum of those. Excellent agreement between simulated and measured spectra is achieved, suggesting that the assumption of mutual thermal equilibrium is valid, at least under optical excitation.

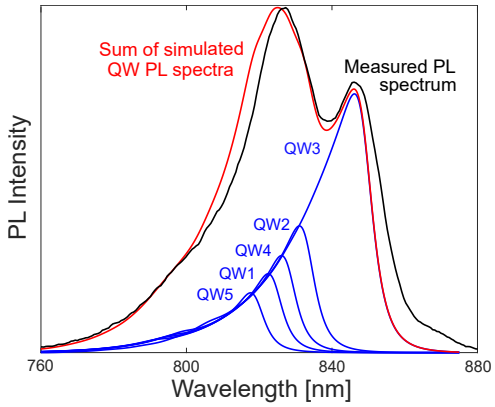

Fig. 2. Simulated RT PL spectra for the different In-content QWs (blue) and the sum of those (red) under the assumption of mutual thermal equilibrium. Measured RT PL spectrum (black).

Standard procedures were used to fabricate VCSELs with a primary oxide aperture diameter of 6 µm. A thick layer of BCB is used under the bond pad to reduce pad capacitance. For testing, an MPI TS200-SE probe station was used to enable measurements from −40 to 125 °C in a moisture-free environment.

III. Static Characteristics

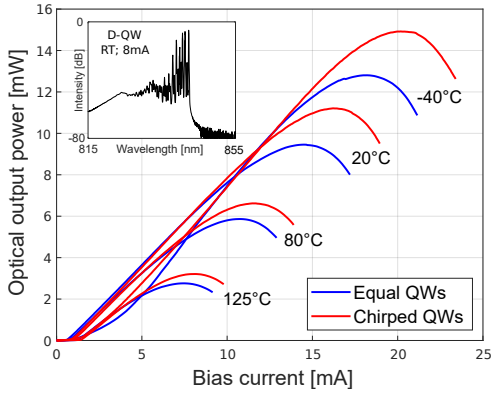

Fig. 3. Output power vs. current characteristics for 6 µm aperture VCSELs with chirped QWs (red) and equal QWs (blue) at different temperatures. The inset shows the RT emission spectrum at 8 mA from the VCSEL with chirped QWs.

This article has been accepted for publication in IEEE Photonics Technology Letters. This is the author's version which has not been fully edited and content may change prior to final publication. Citation information: DOI 10.1109/LPT.2025.3547156.

Fig. 3 shows the output power vs. current characteristics for the two VCSELs at four temperatures from −40 to 125 °C. The two designs exhibit similar behavior with maximum output power and roll-over current decreasing linearly with temperature. Differences can be explained by small but different deviations from the 6 µm nominal aperture diameter. The RT emission spectrum in the inset illustrates the multimode behavior of VCSELs with this aperture size.

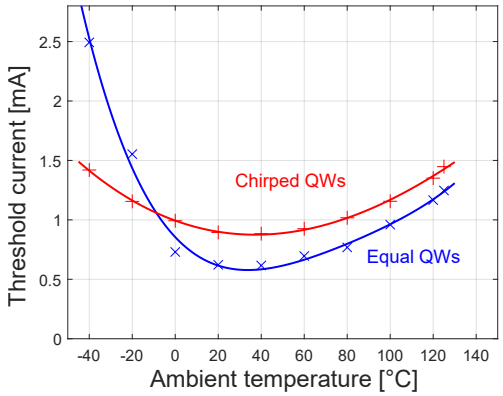

Fig. 4. Threshold current vs. temperature for VCSELs with chirped QWs (red) and equal QWs (blue). Experimental results are shown as data points, with a solid curve representing a polynomial fit to the data.

More interesting is the comparison of threshold current over temperature, shown in Fig. 4. Both VCSELs have minimum threshold current in the middle of the temperature range (at approximately 40 °C). The VCSEL with chirped QWs has a minimum threshold current of 0.88 mA, which increases by only 65% (to 1.45 mA) at the end points of the temperature range. In contrast, the VCSEL with equal QWs, although having somewhat lower threshold current at temperatures above 0 °C, shows a much larger dependence on temperature with excessive threshold currents at the lowest temperatures. While a smaller detuning would reduce the low temperature threshold currents for this VCSEL, it would lead to excessive threshold currents at the highest temperatures. The higher threshold current at most temperatures for the VCSEL with chirped QWs is a direct consequence of the broadening of the optical gain which calls for a trade-off between minimizing threshold at a certain temperature and minimizing variation of threshold current over temperature.

At the lowest temperatures, where the difference between gain peak(s) and resonance wavelengths is largest, the onset of lasing occurs through oxides modes, as confirmed by spectral measurements. Oxide modes can be suppressed by positioning the primary oxide apertures at a node of the optical fields, which is not the case here. The second kink in the IP-curve, which defines the onset of aperture modes, was used as a measure of threshold current.

IV. Dynamic Characteristics

Fig. 5 shows the small signal modulation response (S_{21}) of the two VCSELs at various temperatures and 7 mA bias, measured with the same setup as in [9], together with fits of a three-pole transfer function representing the intrinsic VCSEL response and effects of parasitics [11].

From the measured modulation response, the dependencies of the −3 dB bandwidth and response overshoot on current and temperature were extracted. Fig. 6 shows bandwidth vs. ambient temperature at different bias currents. While the VCSEL with equal QWs has more than 4 GHz higher maximum bandwidth at 7 mA, its bandwidth varies more strongly with temperature. At 7 mA, the VCSEL with chirped QWs has a maximum bandwidth of 22 GHz at 20 °C, which drops by only 2.5 GHz at −40 °C and 5.2 GHz at 125 °C. Such bandwidths should allow for 25 Gb/s NRZ signaling over temperature at constant bias current.

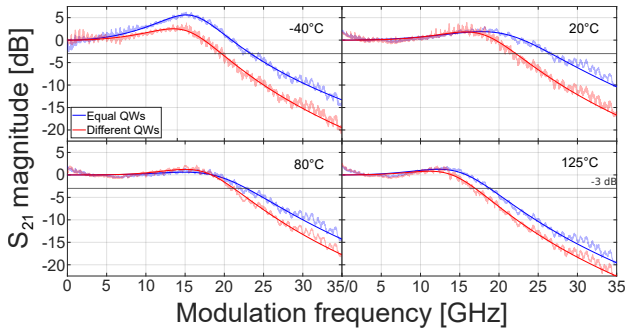

Fig. 5. Modulation response measured at 7 mA bias at different temperatures for the VCSEL with chirped QWs (red) and the VCSEL with equal QWs (blue). Noisy data represents measured modulation response, while smooth line is a fit to a three-pole transfer function.

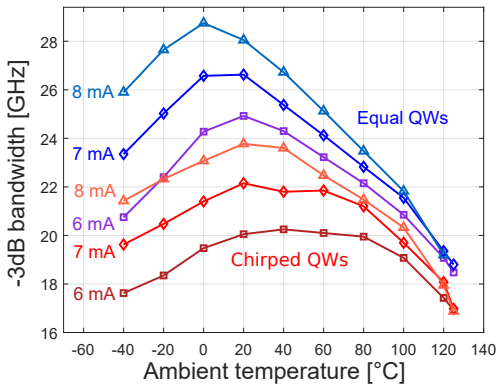

Fig. 6. Bandwidth vs. temperature at various bias currents for the two VCSELs.

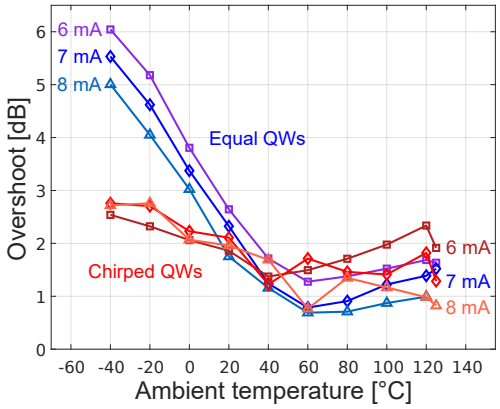

Fig. 7. Modulation response overshoot vs. temperature at various bias currents for the two VCSELs.

This article has been accepted for publication in IEEE Photonics Technology Letters. This is the author's version which has not been fully edited and content may change prior to final publication. Citation information: DOI 10.1109/LPT.2025.3547156.

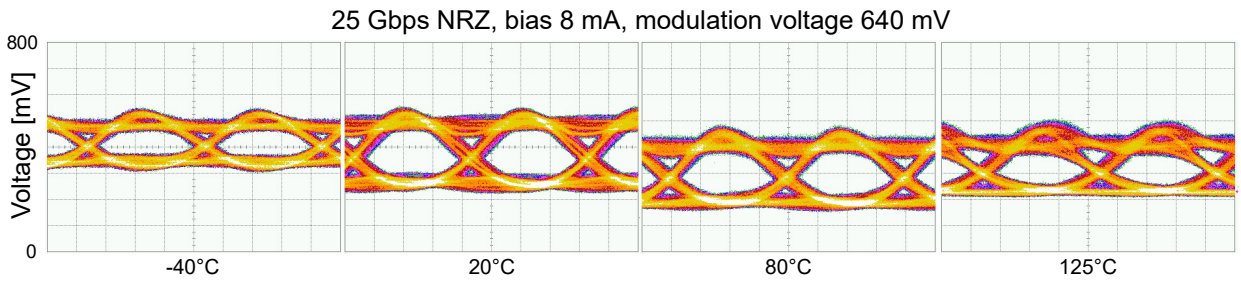

Fig. 8. Eye diagrams at 25 Gb/s NRZ at different temperatures for the VCSEL with chirped QWs, at constant bias current (8 mA) and constant modulation voltage (640 mV). Horizonal scale: 10 ps/div. Vertical scale: 100 mV/div.

Fig. 7 shows the response overshoot vs. ambient temperature at various bias currents. For the VCSEL with chirped QWs, the overshoot is reduced from less than 3 dB at −40 °C to about 1.5 dB at 125 °C at 7 mA bias. On the contrary, the overshoot for the VCSEL with equal QWs exceeds 5.5 dB at the lowest temperature at this current. This is caused by the high threshold current, which reduces the difference between bias and threshold current, and thereby the resonance frequency. When the resonance frequency is reduced to below the parasitic pole frequency, the modulation response becomes more peaked. A large overshoot leads to excessive timing jitter and intersymbol interference which degrades the signal quality under large-signal modulation and data transmission.

V. Data Transmission

To investigate whether the VCSEL with chirped QWs allows for 25 Gb/s NRZ data transmission over the entire temperature range at constant current, we performed large-signal modulation measurements. A 25 Gbaud NRZ signal consisting of pseudorandom binary sequences with a word length of $2^7 - 1$, generated by a bit pattern generator (SHF 12103A), was supplied to the VCSEL through a high-speed bias-T and a high-speed RF probe. The output light was coupled to a lensed OM4 multimode optical fiber, which was connected to a 32 GHz photoreceiver (MACOM PT-28F/MM) via a variable optical attenuator (EXFO FVA-3150). The photoreceiver was connected to a 70 GHz equivalent time sampling oscilloscope (Agilent Infiniium DCA-J 86100C) to capture eye diagrams.

Fig. 8 shows eye diagrams across temperature at a constant bias current of 8 mA and a constant modulation voltage of 640 mV. The open eyes, with limited eye closure due to timing jitter, suggest that 25 Gb/s NRZ transmission is indeed possible at both constant current and constant modulation voltage over the entire temperature range. At the lowest temperature, the vertical eye opening is limited by the higher differential resistance of the VCSEL, which limits the modulation current, while at the highest temperature it is limited by the lower slope efficiency. Ledentsov et al. report slightly better results for QD VCSELs at higher temperatures [7]. However, we demonstrate sufficient performance also at subzero temperatures, using the more mature MQW technology for the active region.

VI. Conclusions

We have presented results from an experimental study of the performance of an 850 nm VCSEL with chirped QWs. The VCSEL is intended for 25 Gbaud data transmission over an extended temperature range. Different composition QWs are used to spectrally broaden the optical gain, with compositions chosen to minimize the variation of threshold current with temperature. This leads to reduced variation of other performance characteristics, such as the modulation response, when the VCSEL is biased at a constant current. We have demonstrated open eyes at 25 Gb/s NRZ back-to-back over the temperature range −40 to 125 °C at constant bias current and modulation voltage.

Acknowledgments

This work was partly performed at Myfab Chalmers. Epitaxial wafers were provided by Jenoptik Optical Systems GmbH.

References

[1] A. Jaffal, P. Boulaya, M. Vallo, and E. Dogmusa, "VCSELs market outlook in consumer sensing and data communication," in *Proc. Vol. 12904, Vertical-Cavity Surface-Emitting Lasers XXVIII*, Mar. 2024, 1290409.

[2] G. N. Liu *et. al.*, "Optical interconnects for intra-vehicle networks: opportunities and challenges," in *2023 Opto-Electronics and Communications Conf. (OECC)*, Jul. 2023, pp. 1-2.

[3] M. Vallo, and P. Mukish, "Global insights into the co-packaged technology platforms enabling transceivers with capacities of 1.6 Tbps and higher," in *Proc. Vol. 12027, Metro and Data Center Optical Networks and Short-Reach Links V*, Mar. 2022, 120270R.

[4] G. G. Ortiz, C. P. Hains, B. Lu, S. Z. Sun, J. Cheng and J. C. Zolper, "Cryogenic VCSELs with chirped multiple quantum wells for a very wide temperature range of CW operation," *IEEE Photon. Technol. Lett.*, vol. 8, no. 11, pp. 1423-1425, Nov. 1996, doi: 10.1109/68.541537.

[5] H.S. Oh *et. al.*, "Realization of broad-spectrum using chirped multi-quantum well structures in AlGaInP-based light-emitting diodes, *J. Nanosci. Nanotechnol*, vol. 21, no.7, pp. 3824-3828, Jul. 2021, doi: 10.1166/jnn.2021.19215.

[6] H. S. Gingrich, D. R. Chumney, S.-Z. Sun, S. D. Hersee, L. F. Lester, and S. R. J. Brueck, "Broadly tunable external cavity laser diodes with staggered thickness multiple quantum wells," *IEEE Photon. Technol. Lett.*, vol. 9, no. 2, pp. 155-157, Feb. 1997, doi: 10.1109/68.553070.

[7] N. Ledentsov *et. al.*, "Quantum-dot oxide-confined 850-nm VCSELs with extreme temperature stability operating at 25 Gbit/s up to 180°C," in *Proc. SPIE 11300, Vertical-Cavity Surface-Emitting Lasers XXIV*, Feb. 2020, 113000H.

[8] P. Westbergh *et. al.*, "High-speed oxide confined 850-nm VCSELs operating error-free at 40 Gb/s up to 85 °C," *IEEE Photon. Technol. Lett.*, vol. 25, no. 8, pp. 768-771, Apr. 2013, doi: 10.1109/LPT.2013.2250946.

[9] H. D. Kaimre, A. Grabowski, J. Gustavsson, and A. Larsson, "Effects of detuning on wide-temperature behavior of 25 Gbaud 850nm VCSELs," in *Proc. Vol. 12439, Vertical-Cavity Surface-Emitting Lasers XXVII*, Mar. 2023, 124390C.

[10] *SimuLase.* Non Linear Control Strategies. [Online]. Available: https://www.nlcstr.com/product/simulase/

[11] L. Coldren, S. Corzine, and M. L. Mašanović, "Dynamic effects," in *Diode lasers and photonic integrated circuits*, Hoboken, NJ, USA: Wiley, 2012, pp. 249–270.